

## Perspective

## Confinement as a Unifying Element in Selective Catalysis

Benjamin Mitschke,<sup>1</sup> Mathias Turberg,<sup>1</sup> and Benjamin List<sup>1,\*</sup>

## SUMMARY

Catalysis has fascinated scientists for centuries and is one of the main pillars of the modern world economy. Achieving high reactivity and selectivity is a crucial requirement of heterogeneous and homogeneous organic, metallic, and biological catalysts. Here, we highlight an underlying principle that is relevant to the reactivity and selectivity of all types of catalysts—"confinement," the shaping of a catalyst's active site. While this aspect has been well recognized within the fields of heterogeneous and enzymatic catalysis, and has been invoked in supramolecular systems, confinement has been less appreciated in the design of small-molecule catalysts. We identify confinement as a unifying element in the science of selective catalysis, reaching beyond the traditional boundaries of the individual subfields. A particular emphasis is given to the latest developments in the area of organocatalysis.

## INTRODUCTION

The term "catalysis" was first dubbed more than 200 years ago and was conceptualized by Berzelius as "to awaken affinities (between chemical reaction partners), which are asleep at a particular temperature."<sup>1</sup> Since then, catalysis has come a long way from the observation of reaction acceleration to a field of research, which is also one of the main drivers for technological innovation. Estimates suggest that 80%–90% of all chemical processes, eventually resulting in fuels, pharmaceuticals, and materials for ubiquitous applications, are catalyzed, and contribute to over one-third of the global gross domestic product.<sup>2</sup> To be useful, however, catalysis needs to be selective.

Thermally and chemically robust heterogeneous catalysts, which dominate industrial applications, frequently achieve high selectivity due to a very specific feature—a confined reaction site. Highly reactive functional groups that are spatially distributed over just a few nanometers within the catalyst framework often enable excellent levels of selectivity and product stability.

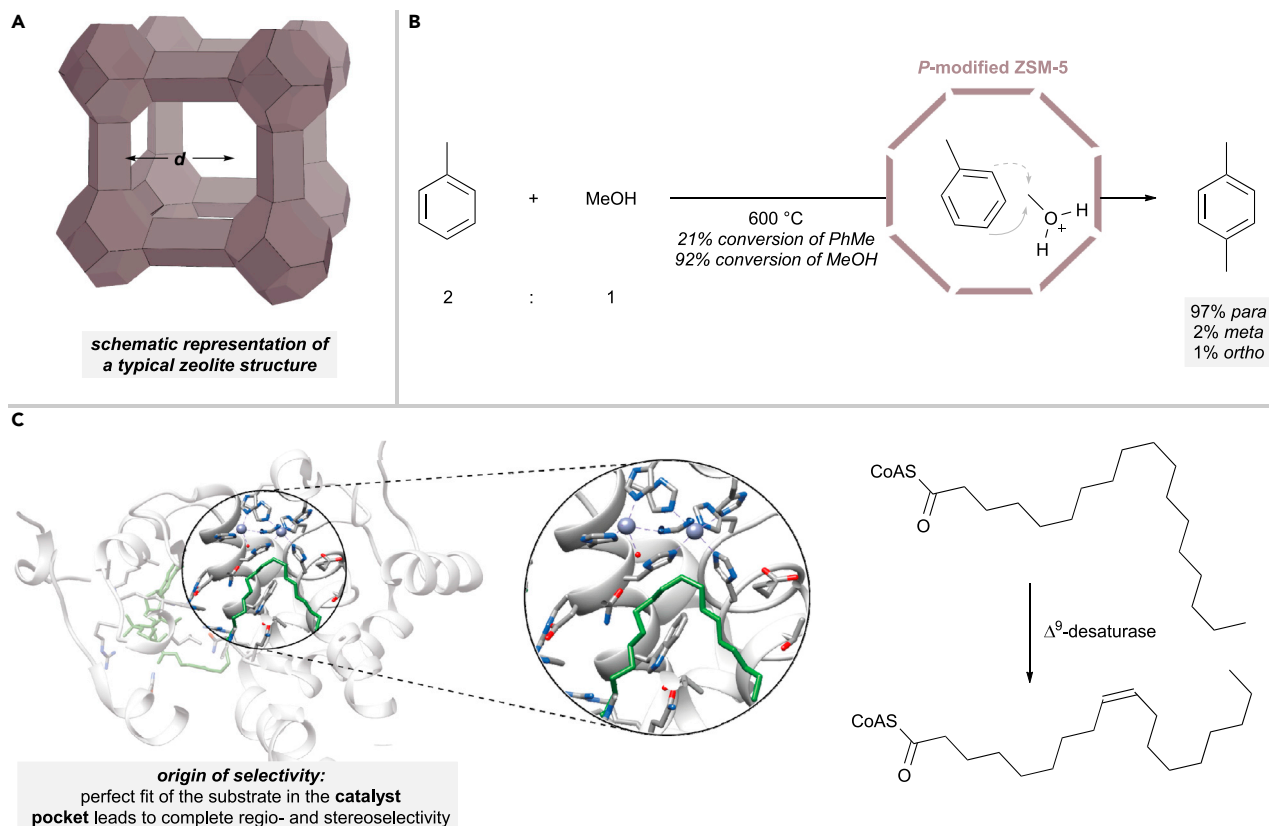
In general, basic atomic properties drastically change upon confinement within the catalyst framework, leading to effects such as increased excitation energy and lower polarizability, which can be explained using the "particle in the box" as a simplified model.<sup>3</sup> For larger molecules, spectroscopic evidence for an intrinsic decrease in the  $\pi$ - $\pi^*$  gap in aromatic hydrocarbons such as naphthalene and anthracene has been shown and was computationally supported by Márquez, García, and Corma.<sup>4–7</sup> More recent studies, however, revealed that the pure effect of confinement rather leads to an increase in the HOMO-LUMO gap and point toward the specific properties of electrostatic stabilization within the active catalytic site—a unique consequence of the confined active center.<sup>8,9</sup>

## The Bigger Picture

Challenges and opportunities:

- Catalysis has contributed massively to our modern-day society. To be selective and reactive catalysts can use "confinement" as a fundamental principle.
- Confinement, which has traditionally been invoked in the context of heterogeneous catalysis, is identified as a key feature of all types of catalysts, including biological, supramolecular, transition metal complex, and organic molecule-based ones.
- Recognition of this concept in every field of catalysis may enable the development of artificial enzymes for the future, culminating in unparalleled selectivities paired with extreme reactivity.





### Scheme 1. Heterogeneous Confined Catalysts, Enzymes, and Substrate-Directed Selectivity

(A) Schematic illustration of a typical zeolite solid-state structure.

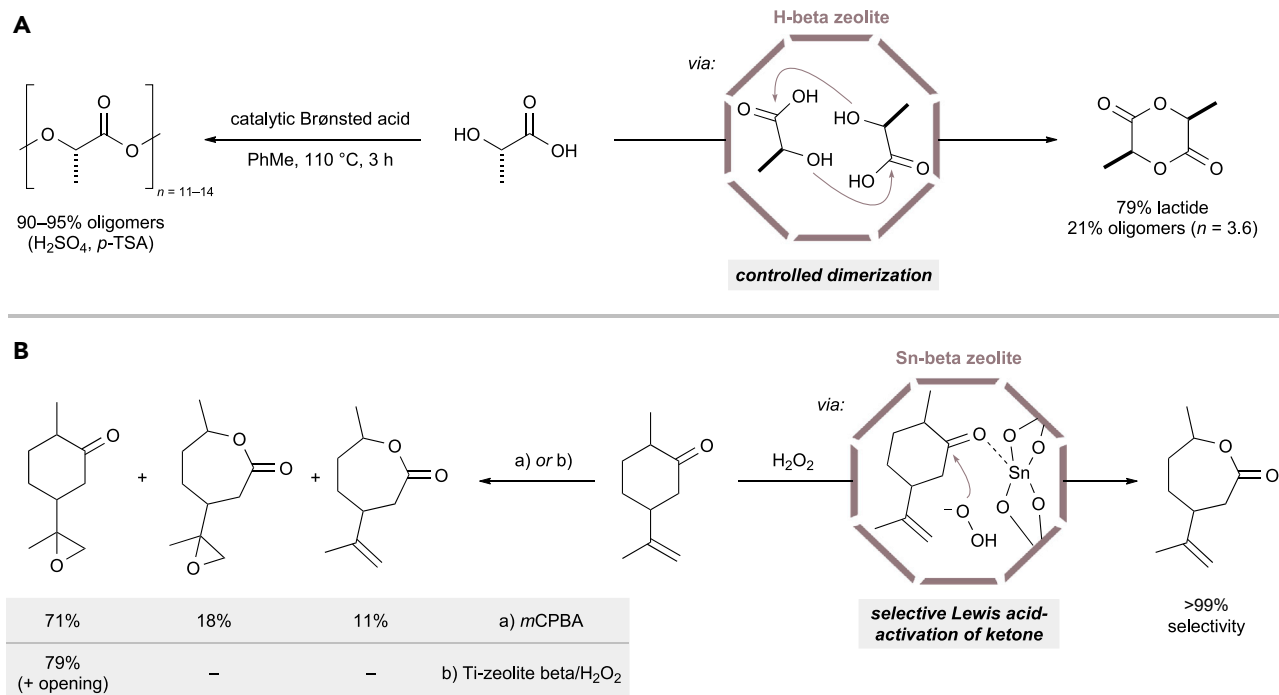
(B) Shape-selective methylation of toluene by *P*-modified ZSM-5.<sup>12,13</sup>

(C) Crystal structure of human stearoyl-CoA desaturase in complex with substrate demonstrates complete catalyst control over regio- and diastereoselectivity (PDB: 4ZYQ).<sup>14</sup>

These results clarify that the unique features of the active site of the catalyst combined with substrate-specific association are key requisites for enhancing both reactivity as well as selectivity. For example, early investigations of zeolites have led to the first description of shape selectivity, i.e., the preference of a catalyst to convert molecules of a certain shape. A phosphorus-modified zeolite was shown to override the thermodynamic distribution of xylene isomers and almost exclusively produce *para*-xylene in the regioselective alkylation of toluene with methanol (Scheme 1B).<sup>10–13</sup> Whereas control of the pore size of heterogeneous catalysts can lead to shape-selective reactions,<sup>10</sup> the active site of an enzyme can be even more well defined and, thanks to an evolutionary refinement, can, in extreme cases, bind and selectively activate only a single substrate. Enzyme-catalyzed reactions often feature the additional aspect of the chiral confinement, i.e., the selection of one enantiomer over the other. The combination of near diffusion-controlled reactivity, paired with an extraordinary level of selectivity, often providing virtually pure isomers, as displayed by many enzymes, signifies the highest degree of sophistication for any type of catalyst.<sup>14–18</sup> One example of this complete catalyst control is the regio- and stereoselective dehydrogenation of stearic acid mediated by the  $\Delta^9$ -desaturase, as shown in Scheme 1C. The substrate is arranged in such a way that the *s-cis* conformation at the 9-position of the aliphatic chain dominates, eventually leading to the pure (*Z*)-diastereomer of an oleic acid derivative.

<sup>1</sup>Max-Planck-Institut für Kohlenforschung,  
Kaiser-Wilhelm-Platz 1, 45470 Mülheim an der  
Ruhr, Germany

\*Correspondence: [list@mpi-muelheim.mpg.de](mailto:list@mpi-muelheim.mpg.de)  
<https://doi.org/10.1016/j.chempr.2020.09.007>



**Scheme 2. Confined Zeolite-Catalyzed Reactions in Comparison with Simple Homogeneous Reagents**

(A) Shape-selective L-lactic acid dimerization catalyzed by H-beta zeolite.<sup>23</sup>

(B) Chemoselective Baeyer-Villiger oxidation of dihydrocarvone.<sup>24</sup>

In homogeneous chemical catalysis, the catalyst typically determines the turnover frequency of a given transformation. Selectivity, in contrast, often requires pre-functionalized substrates. Scientists working in the field of homogeneous catalysis have recently begun to embrace the concept of confinement toward liberating themselves from substrate control and achieve catalyst-controlled selectivity.

### Heterogeneous Catalysts as Robust but Hard to Predict Platforms

In the late 1960s, the catalytic potential of microporous aluminosilicates, especially their rare earth-exchanged variants, was recognized in a variety of Brønsted acid-catalyzed transformations, such as Beckmann rearrangements<sup>19</sup> and electrophilic aromatic substitutions.<sup>20,21</sup> These early results highlighted the vast potential of tailored zeolites as catalysts for numerous transformations.

Poly(lactic acid) is one of the most widely used renewable and biodegradable plastics, and can be synthesized in a controlled manner starting from lactide, the dimer of lactic acid, via ring-opening polymerization. The economic feasibility of this process, however, is strictly limited by the availability of lactide.<sup>22</sup> In 2015, Sels and coworkers demonstrated the controlled dimerization of L-lactic acid mediated by H-beta zeolite (Scheme 2A).<sup>23</sup> Whereas the reaction with simple Brønsted acids such as *para*-toluenesulfonic acid and sulfuric acid yielded unselective oligomerization, refluxing an aqueous solution of lactic acid in toluene in the presence of catalytic amounts of the zeolite gave 79% yield of the desired L,L-lactide.

The combination of a confined reaction site with high Lewis acidity was impressively shown by Corma and coworkers, who employed a Sn-beta zeolite for the chemoselective oxidation of several ketones (Scheme 2B).<sup>24</sup> The reaction of dihydrocarvone

with electrophilic *m*CPBA led to mixtures of both the Baeyer-Villiger product and the epoxide resulting from oxidation of the electron-rich olefins. Interestingly, incorporation of titanium within the framework of the beta zeolite exclusively epoxidized the olefin moiety accompanied by side reactions from epoxide opening, whereas the Sn-beta zeolite demonstrated complete selectivity for the 7-membered lactone. The authors reasoned the origin of selectivity to lie in the preferred activation of the ketone carbonyl group and could be supported by *in-situ* IR spectroscopic comparison to the respective V- and Ti-zeolites.

In the last two decades, enormous progress has been made in the development of metal-organic frameworks (MOFs)<sup>25</sup> and covalent-organic frameworks (COFs)<sup>26</sup> as artificial porous materials that show potential for similar behavior as that of other confined solid-state catalysts, while potentially displaying advantages such as tunability of specific properties. Compared with the numerous applications of zeolites, the use of MOFs and COFs in selective catalysis, however, is more recent.<sup>25–28</sup> Despite the power of *in-situ* analytics, elucidating the exact factors that govern reactivity and selectivity in heterogeneous systems is inherently limited.

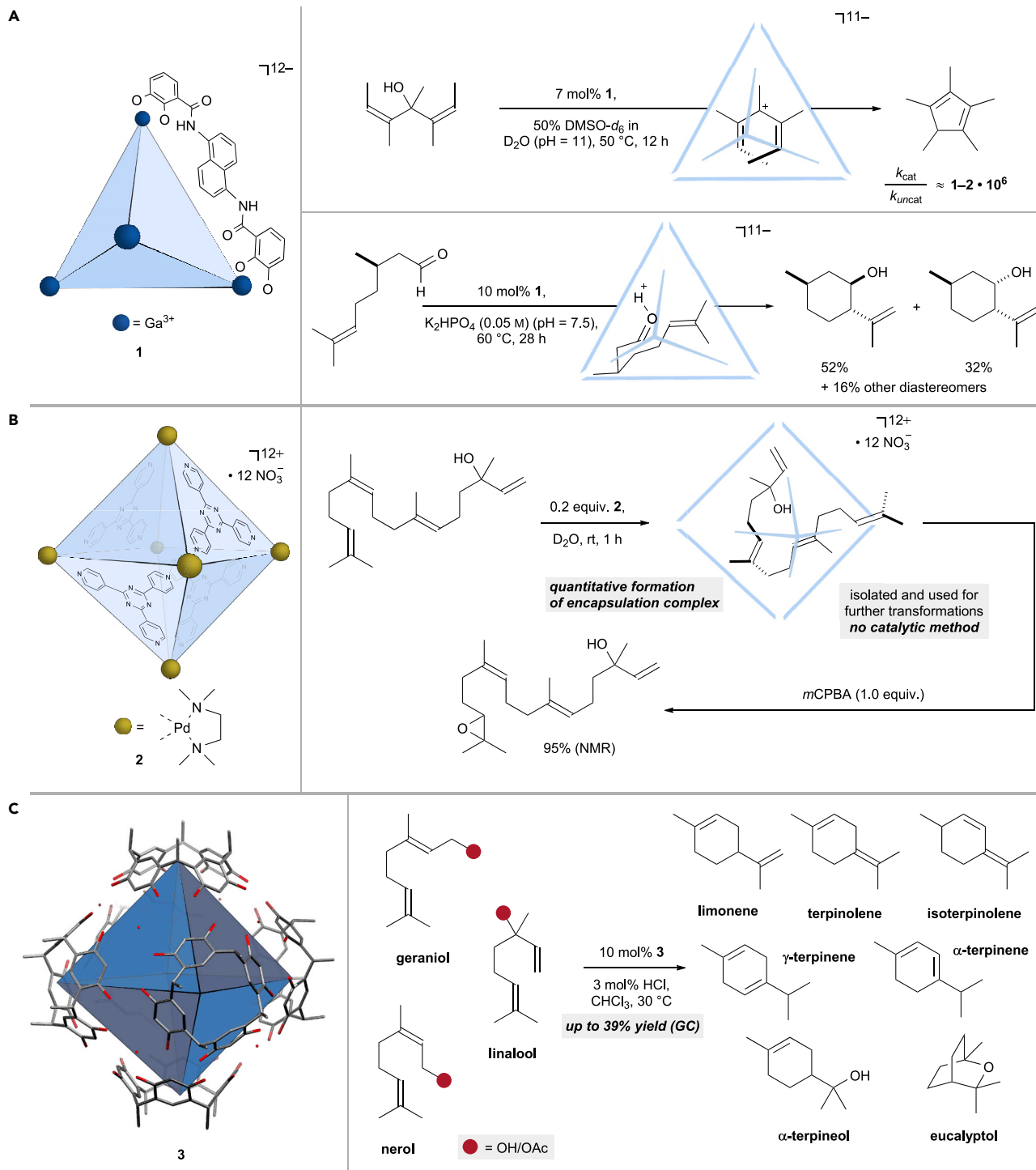
### Confined Reaction Sites in Homogeneous Supramolecular Catalysis

For heterogeneous catalysts, the reactivity is typically determined by the diffusion of a substrate through pores, while the activation is accomplished by the action of functionalities within these pores. Supramolecular assemblies offer similar possibilities, and are accompanied by higher degrees of freedom due to the homogeneous nature of the reaction mixture. It is the sum of the covalent and, often even more important, non-covalent interactions of the homogeneous catalyst with the substrate, sometimes also termed as “second coordination sphere effects,” that determine the exact outcome of a certain catalytic reaction.<sup>29</sup> As a result, a plethora of classes of supramolecular toroids such as cyclodextrins, cucurbiturils, and calixarenes, as well as container- and capsule-like structures have been developed, which enable a wide scope of reactions. The foundation of this field of catalysis was already constructed in the late 1960s by Breslow who recognized the potential of supramolecular catalysts as “artificial enzymes.”<sup>30,31</sup>

As many of the elegant innovations in supramolecular catalysis have been the topic of several review articles,<sup>33–35</sup> here, we cover a short selection of the most recent contributions from the last decade.

In 1998, Raymond and coworkers introduced the self-assembled, anionic  $[\text{Ga}_4\text{L}_6]^{12-}$  cage and demonstrated the efficient encapsulation of ammonium ions (Scheme 3A).<sup>36</sup> The specific naphthalene-bridged chatecholamide ligand is represented by the edges of the highly symmetrical tetrahedron; each vertex corresponds to a single Ga(III) ion. Due to the anionic nature of the cluster and the resulting water solubility, a hydrophobic pocket is created, which readily incorporates organic guests. Additionally, the high negative charge density within the cage leads to a clear preference for cationic guests. In fact, it has been shown that this self-assembled cluster is able to perform Brønsted acid-catalyzed reactions in basic aqueous media.<sup>37,38</sup>

This concept of Brønsted acid catalysis under basic conditions has been developed further by Bergman, Raymond, and coworkers. Traditionally, the Nazarov cyclization is the Lewis or Brønsted acid-catalyzed  $4\pi$ -electrocyclization of divinyl ketones to give cyclopentenones. The groups of Bergman and Raymond found high reactivity in a dehydrative Nazarov cyclization of all diastereomeric 1,3-pentadienols to exclusively give pentamethylcyclopentadiene (Scheme 3A).<sup>39</sup> Even more



**Scheme 3. Highly Selective Transformations as a Result of Encapsulation into Self-Assembled Cages**

(A) Nazarov cyclization and Prins-type reaction catalyzed by  $[\text{Ga}_4\text{L}_6]^{12-}$  cage.<sup>39,40,41</sup>

(B) Selective epoxidation of the diterpene tail protruding from the supramolecular cavity.<sup>42</sup>

(C) Resorcinarene capsule-catalyzed terpene cyclizations.<sup>43–46</sup>

interestingly, the authors noticed an extreme rate acceleration upon encapsulation into the tetrahedral cluster, giving an increase in the rate constant of six orders of magnitude. Previously, aza-Cope rearrangements catalyzed by **1**, displayed a 1,000-fold rate increase, which could be attributed to effective preorganization of the substrate.<sup>47</sup> The significant acceleration of the Nazarov cyclization might be the sum of increased basicity of the hydroxy moiety, leading to an effective dehydration, preorganization of the substrate to populate the reactive *s-cis*-conformation, and an efficient stabilization of the cation. Notably, modulating interactions of the catalyst with an allylic cation comprised of only carbon and hydrogen was achieved. In a later study, it was found that cage **1** is able to regioselectively deprotonate the allylic cation after  $4\pi$ -cyclization at one of the symmetrically identical *exo*-methyl groups depending on the relative configuration of this cationic species.<sup>40</sup>

Toste, Bergman, Raymond, and coworkers also applied the dodecaanionic cluster **1** in a carbonyl ene cyclization of citronellal.<sup>41</sup> The challenge of this transformation does not only lie in the stereochemical outcome but also in competing the side reactivity of the initial products. For example, the reaction of citronellal with aqueous  $\text{KH}_2\text{PO}_4$  (pH = 3.2) led to the formation of 91% of a product, resulting from the Markovnikov-hydration of the isopropenyl group. The extraordinary selectivity of the Ga(III) cluster, however, was demonstrated by using just slightly altered reaction conditions (pH = 7.5) in the presence of 10 mol % of **1**. The isopulegol diastereomers were formed in 97% selectivity with a clear preference for isopulegol with 52% yield.

Scheme 3B depicts one of the many valuable contributions made by the group of Fujita. The self-assembled octahedral cage **2** consists of six Pd(II) ions on each vertex, cross-linked by fairly electron-poor 2,4,6-tri(pyridin-4-yl)-1,3,5-triazine ligands on half of the octahedral faces. The low electron density of the whole coordination cage allows for efficient incorporation of especially electron-rich guests, enabling reaction facilitation by privileging certain conformations of the substrate within the cage. Therefore, it is not surprising that the linear diterpenoid geranylinalool was included into **2** in quantitative yield; similar coordination complexes could be characterized by X-ray crystallographic analysis.<sup>42</sup>

This structural analysis clearly revealed the diterpenoid tail to be protruding from one face of the octahedral cage. As a result, when subjecting the encapsulation complex to several electrophilic reagents, such as *N*-bromosuccinimide (NBS) or *meta*-chloroperoxybenzoic acid (mCPBA), the terminal prenyl group was the exclusive site of reactivity. It has to be noted that these reactions were not performed under catalytic conditions. They still demonstrate the general concept of a confined reaction site and the underlying possibilities associated with it.

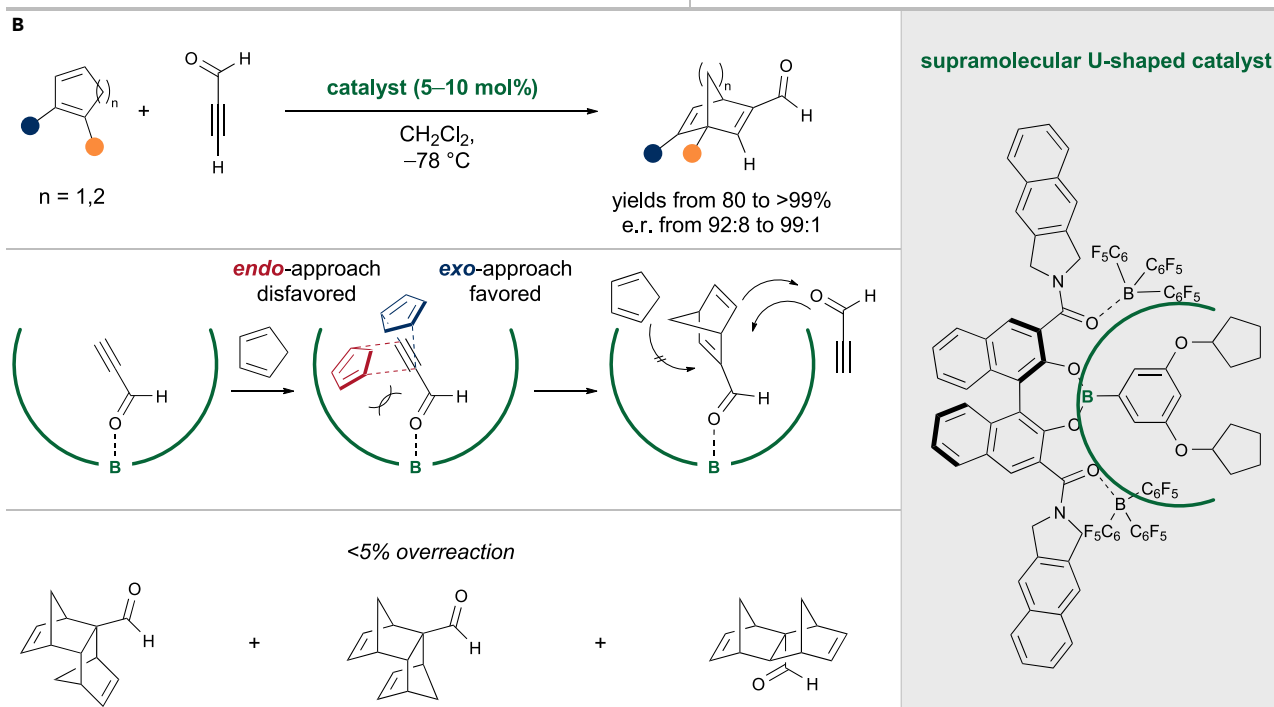
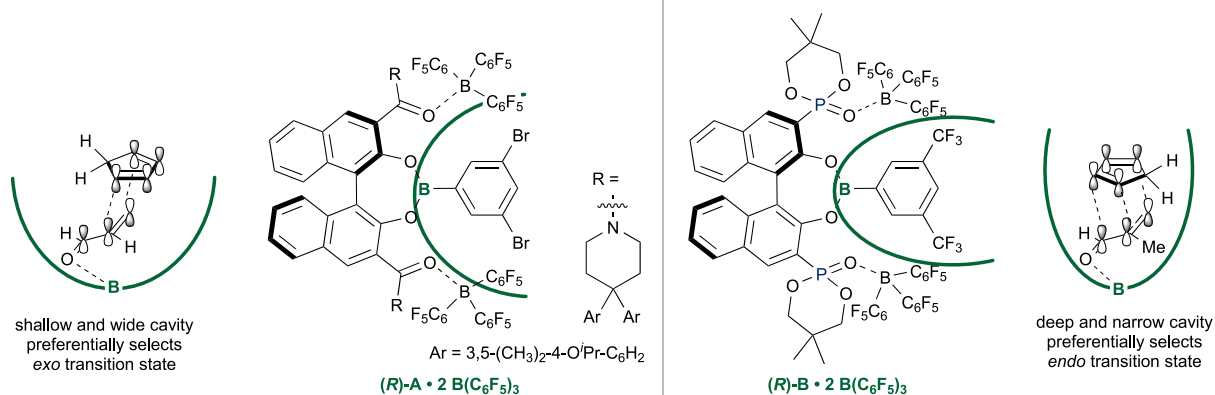
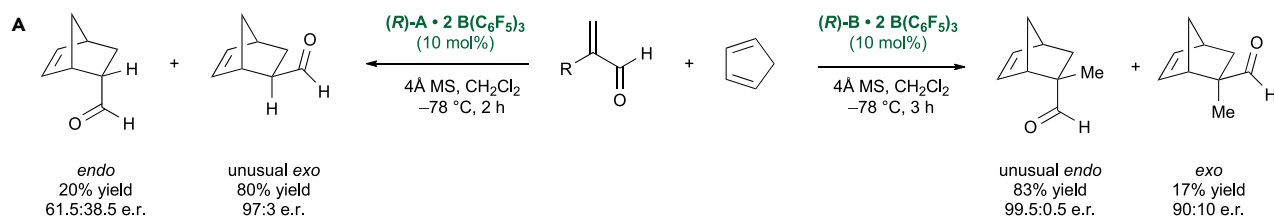
In addition to the aforementioned examples of self-assembled supramolecular reaction vessels, Tiefenbacher and coworkers recently harnessed the confined reaction space of a previously reported resorcinarene capsule<sup>48</sup> to accomplish selective tail-to-head mono-<sup>43</sup> and sesquiterpene cyclizations (Scheme 2C).<sup>44–46</sup> Whereas enzyme-catalyzed tail-to-head terpene cyclizations (THT) typically proceed with extraordinary product selectivities and enantioselectivities, these reactions have proven to be exceptionally difficult to mimic with artificial catalysts and with comparable selectivities. The available crystal structures of type I cyclase enzymes reveal important structural features accounting for the observed high selectivities: (1) aspartate-rich segments serve as binding sites for a divalent metal cation (typically  $\text{Mg}^{2+}$ ), (2) basic residues (such as arginine and lysine) are proposed to stabilize the pyrophosphate leaving group through electrostatic interactions and hydrogen

bonding, (3) aromatic side chains contribute to the stabilization of reactive cationic intermediates via cation- $\pi$  and cation-dipole interactions, (4) recognition and preorganization of the substrate inside a well-defined hydrophobic binding pocket limits the number of accessible conformations, and (5) access of other nucleophiles to the substrate is blocked by the confined reaction space, minimizing premature quenching of reactive intermediates.<sup>49–52</sup> As the initial ionization step in type I cyclases proceeds from a pyrophosphorylated substrate under neutral conditions, potential Brønsted acid-catalyzed side reactions of either the olefin-containing substrate or products are prevented. This unselective side reactivity is commonly observed for linear terpene cyclization precursors requiring acidic conditions.

Toward mimicking the confined reaction space in cyclase enzymes, Tiefenbacher and coworkers identified the hexameric resorcinarene capsule (Scheme 3C) as a suitable supramolecular reaction vessel, which shares key similarities with type I cyclase enzymes. The large hydrophobic cavity (approximate volume of 1,400 Å<sup>3</sup>) of the self-assembled capsule allows for the encapsulation of linear mono- and sesquiterpene cyclization precursors, while, at the same time, forcing the substrate into a folded conformation and preventing side reactions with undesired nucleophiles. Stabilization of cationic intermediates and transition states is proposed to occur via cation- $\pi$  interactions, with the electron-rich aromatic resorcinarene walls. Upon addition of catalytic amounts of HCl and subsequent protonation of the capsule, it is sufficiently acidic to initiate THT cyclization cascades.<sup>53</sup> Indeed, capsule-catalyzed THT cyclizations are remarkably selective, culminating in the efficient synthesis of complex cyclized terpenes that were previously inaccessible under typical reaction conditions in solution, lacking a supramolecular reaction vessel.<sup>43–46</sup> For example, reaction of the common monoterpenes within **3** led to selectivity of up to 39% of the cyclized product depending on the double-bond geometry and/or leaving group, thus requiring some degree of substrate preorganization. However, Tiefenbacher and coworkers suggested that an adequately tuned cavity shape of the capsule might allow for a more efficient substrate preorganization, thus leading to higher product selectivities.<sup>44</sup>

Using a different approach, Ishihara and coworkers reported the development of conformationally flexible chiral BINOL-based boron Lewis acids possessing a specifically designed cavity (Scheme 4).<sup>54–56</sup> Whereas the *endo/exo* selectivity in Diels-Alder reactions is typically governed by the structure of the substrates, synthetic access to the respective unpreferred diastereomer is difficult to attain. However, Ishihara and coworkers demonstrated that a catalyst with an appropriately designed cavity is capable of accelerating the formation of the anomalous diastereomer. Structurally, the authors classified the developed catalysts to reside between small-molecule catalysts and rigid supramolecular structures such as MOFs. More specifically, the *in-situ* generated supramolecular catalysts involve the coordination of two additional boron-based Lewis acids to Lewis-basic sites of the chiral BINOL-derived fragment. Computational studies suggest that a deep and narrow cavity of the Lewis acid prefers the unusual *endo* isomer over the sterically preferred *exo* isomer in the case of  $\alpha$ -substituted dienophiles. In the case of unsubstituted  $\alpha,\beta$ -unsaturated aldehydes, a Lewis acid with a shallow and wide cavity preferentially selects the *exo* over the electronically preferred *endo* isomer (Scheme 4A).

Very recently, the benefit of a confined reaction site was further showcased in the application to an unprecedented multiselective Diels-Alder reaction of propargyl aldehyde with a variety of dienes (Scheme 4B).<sup>56</sup> The formed norbornadiene cycloadducts are prone to overreaction, as the second Diels-Alder reaction outcompetes



**Scheme 4. Supramolecular Catalytic Asymmetric Transformations Using Confined Reaction Sites**

(A) Overriding the diastereoselectivity in a catalytic asymmetric Diels-Alder reaction between cyclopentadiene and  $\alpha$ -substituted acroleins.<sup>54,55</sup>

(B) The confined reaction site of the U-shaped catalyst prevents side reactions of the norbornadiene product in the Diels-Alder reaction between cyclic dienes and propargylaldehyde.<sup>56</sup>

the first one and exclusively provides the corresponding sesquinorbornadienes. Therefore, the catalyst has to control the substrate selectivity between propargyl aldehyde and the norbornadiene product to prevent undesired overreaction with the diene.

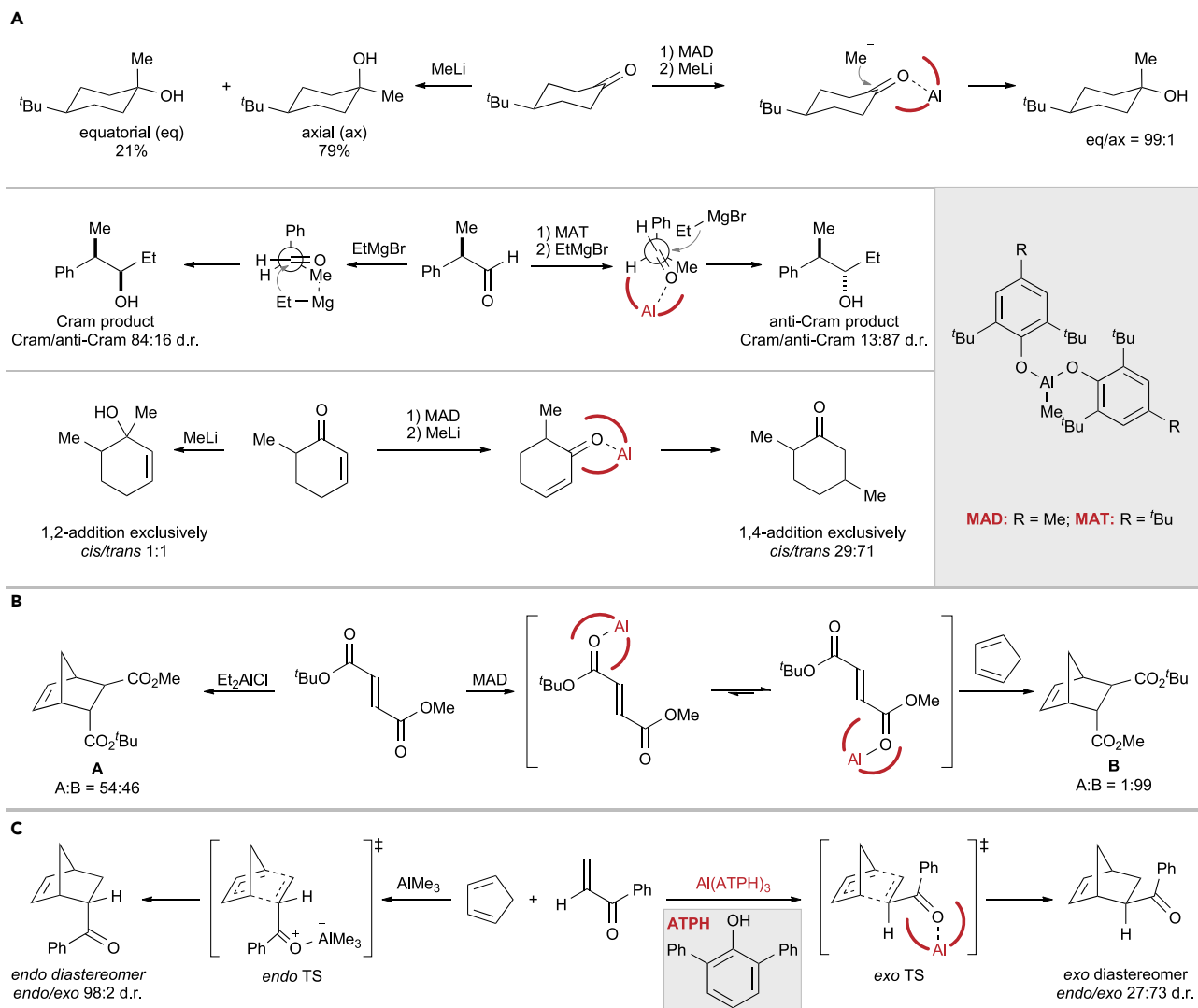
Ishihara and coworkers impressively demonstrated that specifically tailored U-shaped boron Lewis acids impart excellent substrate, *endo/exo*-, regio-, and enantioselectivities in Diels-Alder reactions of different dienes with propargyl aldehyde. Density functional theory (DFT) studies indicated that the size of the cavity preferentially selects the small propargylaldehyde over the much larger norbornadiene Diels-Alder product.

### Confined Small-Molecule Systems in Homogeneous Catalysis

In the previous sections, we hope to have shown that “confinement” is an established concept in the fields of catalysis of higher-order systems, such as solid-state as well as supramolecular catalysts. In small-molecule homogeneous catalysis, however, selectivity has mostly been explained with the specific features of the monomolecular “[chiral] pocket” of the catalyst, as determined by the arrangement of key substituents around the reactive center. This notion led to extensive applications and can often provide a good explanation for observed selectivities based on the ground state conformations of the reactants. In the remaining part of this perspective, we would like to show that the key principles of “confinement,” which lead to the emergence of effects such as shape- and size-selectivity, prevention of side reactions, substrate preorganization, and stabilization of reactive intermediates can indeed be recognized for certain small-molecule catalyst systems. We conclude that the ideal confined catalyst shapes a specific reaction volume that is exclusively complementary to the transition state of the desired transformation by specifically limiting the degrees of freedom of the interacting reactants. It has to be noted that this definition of confinement is, to some extent, different from the bare description of second coordination sphere effects, which has been used for heterogeneous and supramolecular catalysts.<sup>57</sup> Therefore, we recommend caution in the interchangeable usage of (*chiral*) pocket and *confined reaction site* for small-molecule systems since a well-suited reaction center is rather a prerequisite for a catalyst, whereas a *confined* catalyst exhibits additional features that lead to the abovementioned effects.

Examples of this model with small-molecule homogeneous catalysts are relatively scarce. In 1985, Yamamoto published one of the earliest examples demonstrating the influence of a confined reaction space on reaction outcomes, using bulky aluminum-based Lewis acids (Scheme 5). Although the organoaluminum Lewis acids were used as reagents rather than catalysts, the observation that small molecules with tailored cavities were capable of altering product selectivities was conceptually new. For instance, it was shown that carbonyl compounds complexed with exceptionally bulky organoaluminum Lewis acids such as methylaluminum bis(2,6-di-*tert*-butyl-4-methylphenoxide) (MAD), methylaluminum bis(2,4,6-tri-*tert*-butylphenoxide) (MAT), and aluminum tris(2,6)-diphenylphenoxide (ATPH), showed unusual equatorial, *anti*-Cram, and 1,4-addition selectivities in carbonyl alkylation reactions (Scheme 5A).<sup>58,59</sup> The striking difference in selectivity compared with more conventional, less bulky Lewis acids arises from the selection of the sterically preferred isomer of the activated complex. In the case of the high selectivity toward 1,4-addition of organometallic reactions to  $\alpha,\beta$ -unsaturated carbonyl compounds, it was reasoned that the carbonyl group is efficiently shielded from 1,2-addition within the cavity of the formed complex.

Indeed, a crystal structure of the  $C_3$ -symmetric *N,N*-dimethylformamide-ATPH complex later revealed a propeller-like arrangement of the phenoxide ligands surrounding the central aluminum atom, thus creating a buried carbonyl binding pocket.<sup>62</sup> In 1992, the bulky Lewis acids were applied to regio- and stereocontrolled



### Scheme 5. Selective Carbonyl Additions and Stereocontrolled Diels-Alder Reactions by the Means of Bulky Organoaluminum Lewis Acids

(A) Lewis acid-controlled regio- and diastereoselective addition of organometallic reagents to carbonyl groups and Michael acceptors.<sup>58,59</sup>

(B) Exo-selective Diels-Alder reaction between cyclopentadiene and acrylophenone. This reaction is one of the few examples where the aluminum Lewis acid could be used in catalytic quantities (30 mol %).<sup>60</sup>

(C) Size-selective coordination of the organoaluminum Lewis acid leads to complete control over the diastereoselective outcome of this Diels-Alder reaction.<sup>61</sup>

Diels-Alder reactions of fumarates bearing different ester groups (Scheme 5B). An efficient selection of the smaller ester group by the sterically demanding Lewis acid accounted for the observed high selectivities.<sup>61</sup> After two years, Yamamoto demonstrated that the ATPH complex was capable of overriding the preference for the *endo* diastereomer in Diels-Alder reactions of  $\alpha,\beta$ -unsaturated ketones with cyclopentadiene by effectively controlling the approach of the diene (Scheme 5C). The previously unattainable *exo* diastereomer was obtained almost exclusively for  $\alpha$ -substituted  $\alpha,\beta$ -unsaturated carbonyl compounds and in diastereoselectivities of up to 27:73 *endo/exo* for  $\alpha$ -unsubstituted systems. This work is also a rare example of the catalytic application of the aluminum Lewis acids (30 mol % used for a single example).<sup>60</sup> Interestingly, this very concept can also be recognized in the recent work on catalytic asymmetric Diels-Alder reactions by Ishihara that has been discussed earlier.

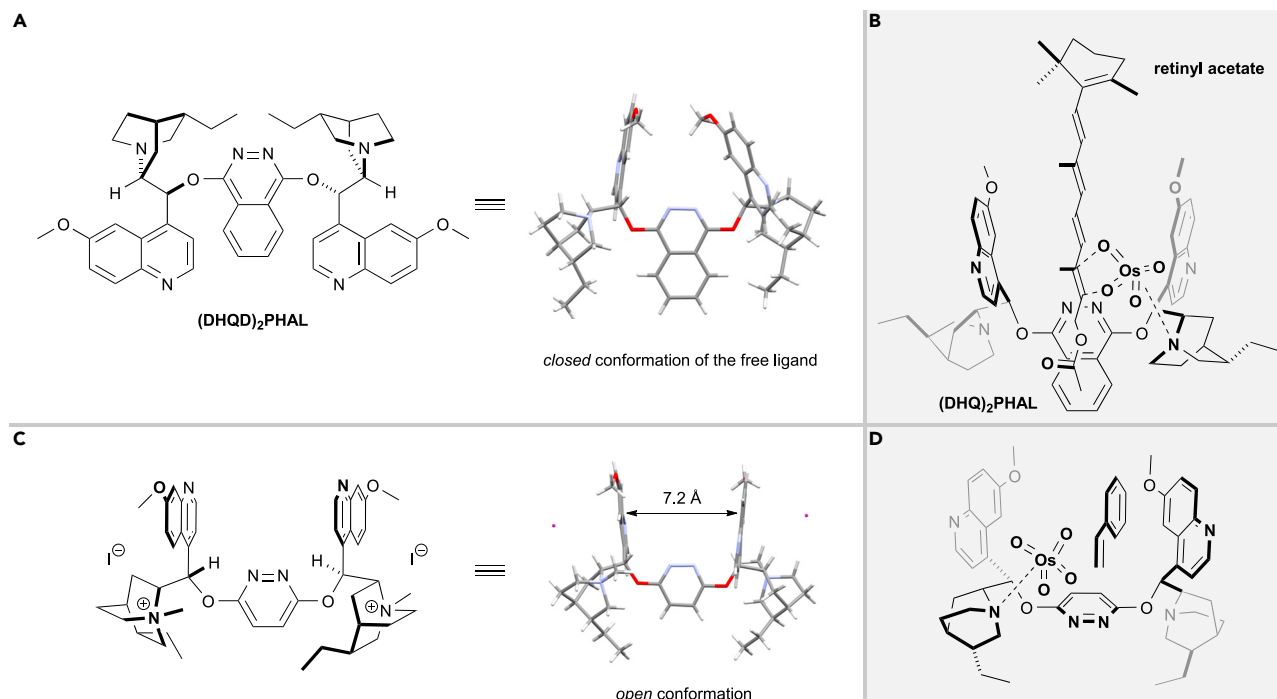


**Figure 1. Structural Information and Proposed Reactive Conformations for the  $\text{OsO}_4$ -Catalyzed Asymmetric Dihydroxylation**

(A) Crystal structure of the bis-cinchona alkaloid-derived phthalazine  $(\text{DHQD})_2\text{PHAL}$  reported by Sharpless.<sup>68</sup>

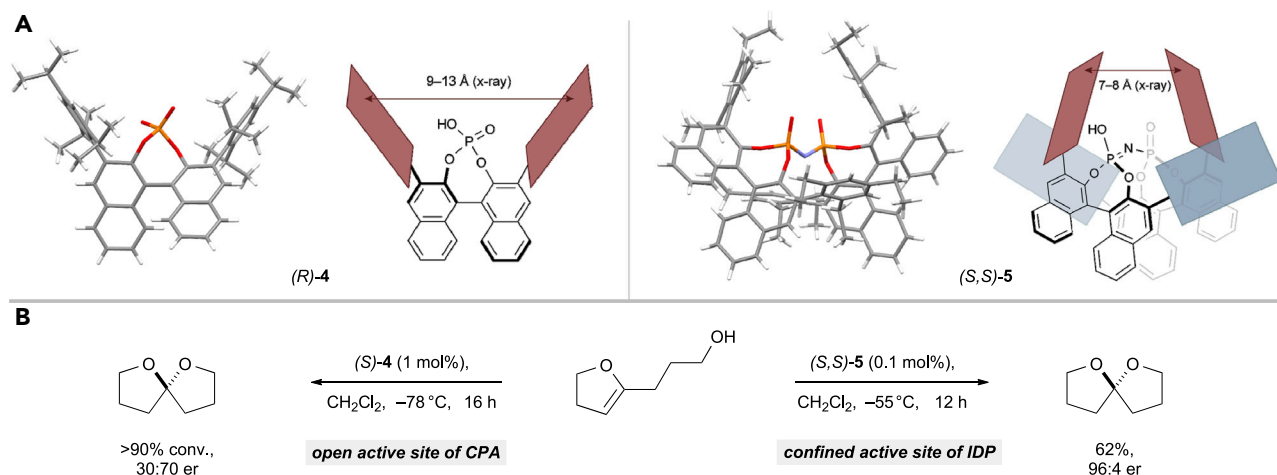
(B) Transition state proposed by Corey for the asymmetric dihydroxylation of retinyl acetate.<sup>69</sup>

(C) Crystal structure of the bisammonium salt of a bis-cinchona alkaloid-derived phthalazine ligand described by Corey.<sup>70</sup>

(D) Proposed binding model for the asymmetric dihydroxylation of styrene.<sup>70</sup>

Catalysts with achiral yet confined active sites have been shown to deliver specifically shaped products with high levels of selectivity in the corresponding non-asymmetric transformations. Enzymes are capable of achieving extraordinary rate enhancements accompanied by astonishing levels of stereoselectivity in asymmetric transformations. Harnessing these properties on homogeneous small-molecule catalysts is arguably one of the most important goals in asymmetric catalysis. Yet, until recently, most asymmetric transformations catalyzed by small molecules rely on pre-functionalization of the substrate to enhance key substrate-catalyst interactions responsible for high levels of stereoselectivity.<sup>63–65</sup>

The asymmetric olefin dihydroxylation, initially reported in 1980 by Sharpless et al. and later improved in 1992, is one of the earliest examples of a homogeneous small-molecule catalyst with a defined molecular cavity capable of transforming a wide range of substrates to the corresponding diols with good-to-excellent enantioselectivities (Figures 1A and 1C).<sup>66,67</sup> Crystallographic studies, molecular mechanics (MM), nuclear magnetic resonance-spectroscopic and kinetic data later revealed the key features of the catalyst.<sup>68–72</sup> Perhaps the most intriguing aspect of the catalytically active complex was the identification of an “enzyme-like U-shaped binding pocket” possessing appropriate dimensions to allow for the inclusion of olefin substrates, which accounts for the high reactivities and enantioselectivities.<sup>68</sup> Notably,  $(\text{DHQD})_2\text{PHAL}$  adopts a closed conformation (Figure 1A) in the solid state, whereas the crystal structure of the bisammonium derivative of a related ligand indicates an open conformation (Figure 1C), highlighting the U-shaped binding pocket created by the two methoxyquinoline rings. The structural studies clearly reveal well-defined binding sites for both  $\text{OsO}_4$  (via the quinuclidine moiety) and the olefin substrate



### Scheme 6. Structural Comparison of the Active Site of TRIP CPA and Confined IDP Catalyst

(A) Comparison of the crystal structures of (R)-TRIP 4<sup>74</sup> and (S,S)-IDP 5.<sup>75</sup>

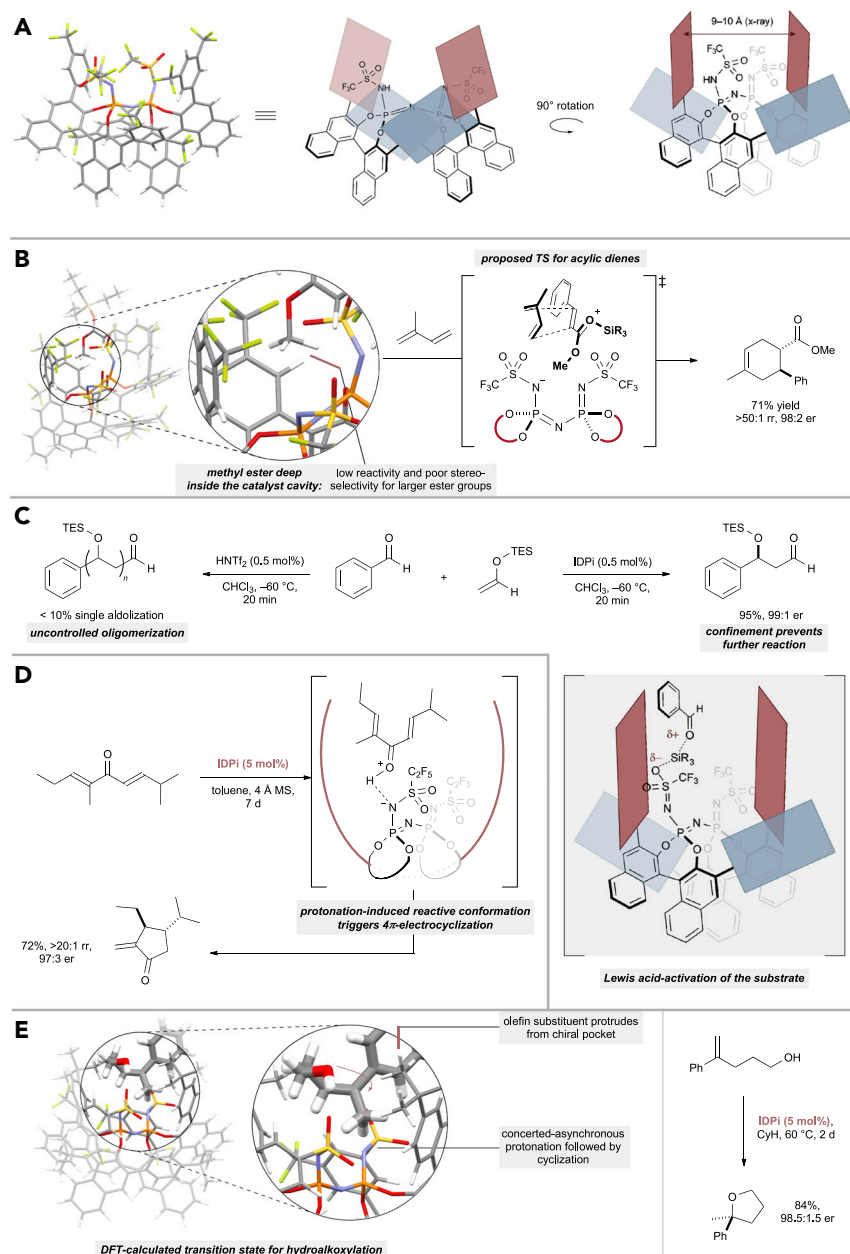
(B) The difference between an open active site in 4 is directly reflected in inferior enantioselectivity compared with the confined Brønsted acid catalyst 5.<sup>70</sup>

(inside the hydrophobic binding pocket via non-covalent interactions, see Figures 1B and 1D) reminiscent to those (binding sites) typically found in enzymes.

In 2012, imidodiphosphates (IDPs) were introduced as confined chiral Brønsted acids. A comparison of the crystal structures of the IDP motif with the analogous chiral phosphoric acid (CPA) clearly shows the striking structural differences between the two scaffolds (Scheme 6). The active site of the CPA is located inside a broad conical-shaped environment of the two 3,3'-substituents of the two 1,1'-bi-2-naphthol (BINOL) fragments. In contrast to this, the active site of the IDP catalysts is deeply buried inside the cavity created by the four 3,3'-substituents. This difference becomes even clearer in the application of both catalysts in the asymmetric spiroacetalization depicted in Scheme 6B.<sup>73</sup> Both reactions lead to full conversion of the dihydrofuran, however, CPA 4 provides the product with only 30:70 er, as compared with the confined IDP catalyst, furnishing the almost enantiomerically pure spiroacetal.

The confined active site confers high levels of stereoinduction in asymmetric transformations even in the case of small and unfunctionalized aliphatic substrates, without additional stereodiscriminating elements. In addition to the steric constraints posed by the IDP catalyst, its acidity increased significantly compared with CPAs ( $pK_a = 11.5$  in CH<sub>3</sub>CN; for comparison: the typical  $pK_a$  of CPAs is in the range of 13–14). Yet, even more reactive catalysts were introduced four years later by replacing the central oxygen atoms in the IDP core with NTf groups, which led to a rather dramatic 10 million-fold increase in acidity of the newly obtained imidodiphosphorimidate (IDPi) Brønsted acids ( $pK_a = 4.5$  to  $\leq 2.0$  in CH<sub>3</sub>CN; see Scheme 7).<sup>76,75</sup>

As with the IDP motif, the crystal structure of IDPi catalyst also exhibits a well-defined binding pocket. Closer inspection indicated that the 3,3'-substituents of the two BINOL fragments create a chiral pocket with a distance between 9 and 10 Å (Scheme 7A). It is the combination of this confined reaction space residing inside a chiral microenvironment with the high reactivity resulting from extraordinary acidity, which enabled the application of this catalyst motif in several challenging and sometimes entirely unprecedented asymmetric transformations.<sup>81</sup>



### Scheme 7. Imidodiphosphorimidates Combine a Confined Reaction Site with High Brønsted and Lewis Acidity in a Single Small-Molecule Catalyst

(A) X-ray crystal structure of a typical IDPi (3,5-bis(trifluoromethyl)phenyl-substitution in the 3,3'-positions of the BINOL backbone; *N*-trifluoromethyl sulfonamide inner core).<sup>75</sup>

(B) DFT-calculated ion pair structure of Lewis acid-activated methyl cinnamate reveals close interaction of the methyl ester moiety with the deep catalyst pocket.<sup>77,78</sup>

(C) Single aldolizations of acetaldehyde-derived enol silanes with benzaldehyde enabled by the highly Lewis-acidic and confined reaction sites of IDPi catalysts.<sup>79</sup>

(D) The confined reactive site of the IDPi catalyst infers the reactive *s-trans/s-trans*-conformation on the substrate to enable a subsequent Nazarov cyclization.<sup>80</sup>

(E) The high acidity of IDPi catalysts is a key requisite for the protonation of simple olefins followed by intramolecular cyclization.<sup>81</sup>

Notably, the reactivity regime of the IDPi catalysts bifurcates into Brønsted acid- as well as Lewis acid-catalyzed transformations; the Lewis acidity is unleashed upon protodesilylation of sacrificial amounts of a suitably basic silyl donor reagent (enol or allyl silanes), forming the corresponding silylium IDPi. In 2018, an enantioselective Diels-Alder reaction of simple unactivated  $\alpha,\beta$ -unsaturated methyl esters with cyclic and acyclic dienes was reported by List et al. (Scheme 7B). Through computational and experimental studies, a conspicuous geometrical match of the IDPi anion and the silylated methyl ester substrate was revealed. Although the model substrate, methyl cinnamate, furnished the desired Diels-Alder product with 1,3-cyclopentadiene in excellent yield and enantioselectivity, the reactions with ethyl and benzyl cinnamate proceeded at a much slower rate, with significantly lower levels of enantioselectivity. This observation is reminiscent of the results obtained by Yamamoto in the regioselective Diels-Alder reaction of unsymmetrically substituted fumarates.<sup>61</sup> In accordance with the experimental data, computational studies suggest that the activated cationic dienophile is deeply buried within the chiral cavity of the counteranion, therefore explaining the preferential recognition of sterically less demanding substrates.<sup>77</sup>

In the same year, an asymmetric single aldolization of acetaldehyde enolates was also achieved by List and coworkers (Scheme 7C). This particular example further validated the aptitude of the confined IDPi catalysts, as the initially formed aldol product is prone to oligomerization with traditional unconfined catalysts. For example, subjecting benzaldehyde and the acetaldehyde-derived enol silane to catalytic amounts of bis(trifluoromethyl)sulfonimide gave only 10% of the desired single aldolization product, along with complex mixtures of oligomers and polymers. A previous approach to circumvent oligomerization of the aldol product involved the use of the exceptionally bulky tris(trimethylsilyl)silyl group that allowed for controlled catalytic non-enantioselective single and double additions.<sup>82,83</sup> The IDPi-catalyzed approach relies on the preferential selection of the less bulky aldehyde substrate over the more congested aldol product in the cavity of the catalyst. Control experiments confirmed that an appropriate steric congestion of the silyl group of the enol silane was required to increase the recognition of the substrate and to minimize oligomerization of the product. Similarly, in the Mukaiyama-Michael reaction, the immediate product after the nucleophilic addition is a silyl ketene acetal. Due to the nucleophilicity of the reaction product, polymerization could occur. Notably, the IDPi-catalyzed Mukaiyama-Michael reaction of  $\alpha,\beta$ -unsaturated methyl esters benefited from the confined activation of the substrate, showing an exclusive single nucleophilic addition by the silyl ketene acetal starting material.<sup>84</sup>

The confinement of the IDPi active site can also play a crucial role in increasing the overall reactivity of a given process, by inducing a more reactive conformation of the chosen substrate. For instance, in a recently reported asymmetric Nazarov cyclization of simple, acyclic divinyl ketones, it is suggested that the IDPi catalyst increases the population of the reactive but more sterically congested *s-trans/s-trans* conformation of the divinyl ketone substrate (Scheme 7D).<sup>80</sup> The resulting cyclopentenone products were released after regioselective deprotonation of the *exo*-methyl group, regenerating the catalyst for further reaction. A similar behavior of the IDPi catalysts could be observed for the intramolecular hydroalkoxylation of simple olefins (Scheme 7E).<sup>81</sup> DFT studies have shown that not only the protonation and subsequent stabilization of the resulting cation by the highly dispersed negative charge of the catalyst anion is necessary for this transformation, but, moreover, preorganization of the substrate in such a way that the activation of the  $\pi$ -bond is directly followed by the intramolecular cyclization within the boundaries of a

concerted yet asynchronous mechanism was shown to be the key requisite for the overall reaction. Interestingly, the substituent of the terminal olefin has been found to protrude from the chiral pocket of the IDPi catalyst. This observation illustrates the high affinity of the pent-4-enol moiety to the catalyst, yielding a broad range of products with excellent enantioselectivities, irrespective of their substitution pattern. For almost every intramolecular cyclization, *gem*-dimethyl substitution on the aliphatic chain bearing the nucleophilic functional group is known to increase the rate of cyclization tremendously. Interestingly, the opposite of this Thorpe-Ingold effect could be observed for the intramolecular hydroalkoxylation. As it is apparent from the DFT-calculated transition state displayed in [Scheme 7E](#), any type of substitution along the aliphatic chain of the reactant would lead to additional steric repulsion with the catalyst pocket. Indeed, a 4-fold increase in reaction time was required to reach a full conversion for such a Thorpe-Ingold substrate.

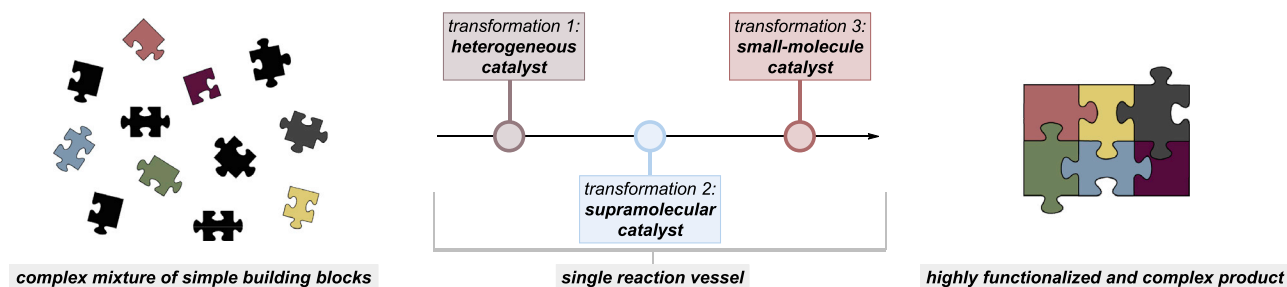
### CONCLUDING REMARKS AND PERSPECTIVE

Confinement had traditionally been discussed in heterogeneous and biological catalytic systems. The combination of a confined active site with reactive functional groups has historically led to rapid advancements in catalysis, enabling unprecedented reactivity and selectivity.

In this overview, we hope to have illustrated that confinement can serve as a logical bridge between zeolites, as naturally occurring heterogeneous catalysts and homogeneous small-molecule catalysts that exhibit their catalytic properties by manifesting this same fundamental property. The bridge was inspired by the catalysts of nature, enzymes, and paved by pioneering work on supramolecular catalysis in the late 1960s and more recently. The confinement concept has also found purpose in non-supramolecular homogeneous systems with bulky aluminum Lewis acids, typically used stoichiometrically.

In recent years, the exploration of small-molecule organocatalysts that combine all of the previously described factors in one structure has finally brought confinement to the attention of homogeneous catalysis. These highly active and extremely confined Brønsted and Lewis acids enabled the selective modification of the smallest substrates in transformations that had previously required sophisticated enzymes or pre-functionalized and engineered substrates. However, it has to be pointed out that these reports also relied on functional groups in the substrates that display some kind of basicity as suitable handle for sufficient interaction. It arguably is the goal of homogeneous catalysis to allow for highly selective transformations of substrates that do not exhibit regions of high electron density and inevitably invokes the specific fine tuning of non-covalent interactions of the catalyst with its substrate, similar to the inspiring arrangement of fatty acid chains within the active site of desaturase enzymes and many more.

Taking a broad view on confinement as unifying element in every aspect of modern catalysis, harnessing the individual advantages of confined reaction spaces could ultimately culminate in processes involving catalysts ranging from heterogeneous over supramolecular to small molecules in a single reaction vessel ([Scheme 8](#)). Ideally, the starting materials will not have to be prepared in a careful and high-yielding manner any more, but could rather be employed as crude mixtures of the simplest building blocks directly obtained from feedstock chemicals. The kinetic preference of a certain catalyst for its substrate will eventually lead to the recognition of a single molecule out of this complex mixture, driving highly selective transformations



**Scheme 8. A Possible Future of Chemical Synthesis**

thereof. This would closely resemble biological systems with a multitude of substrates and enzymes being present in the same cellular compartment, yet, each enzyme specifically recognizes its particular substrate. Highly selective catalysis within complex reaction mixtures immediately raises the question of the origin of substrate specificity for a given catalyst, and confinement could be a promising candidate for an answer. In today's world, every class of catalyst system needs to be prepared and tailored for a certain transformation—a long process of hard labor. Exploiting all of the past and future results in the research of structure-activity relationships of catalysts and combining them with emerging digital technologies, such as artificial intelligence, will enable the rational prediction of catalysts on the basis of pattern analysis perhaps inconceivable for the human mind. The first steps in this direction have already been made, and as a consequence, processes such as the one depicted in [Scheme 8](#), may well become reality in the near future.

## ACKNOWLEDGMENTS

Generous support from the Max Planck Society, the Deutsche Forschungsgemeinschaft (Leibniz Award to B.L. and Cluster of Excellence Ruhr Explores Solvation, RESOLV), Fonds der Chemischen Industrie (Kekulé Fellowship to B.M. and M.T.), and the European Research Council (Advanced grant agreement no. 694228 “C–H Acids for Organic Synthesis, CHAOS”) are gratefully acknowledged. The authors would like to thank Dr. Miles Aukland for help during the preparation of this manuscript.

## REFERENCES

- Berzelius, J.J. (1836). Considerations respecting a new power which acts in the formation of Organic Bodies. *The Edinburgh New Philosophical Journal* 21, 223–238.
- Rothenberg, G. (2008). *Catalysis – Concepts and Green Applications* (Wiley).
- Chattaraj, P.K., and Sarkar, U. (2003). Effect of spherical confinement on chemical reactivity. *J. Phys. Chem. A* 107, 4877–4882.
- Márquez, F., Zicovich-Wilson, C.M., Corma, A., Palomares, E., and Garcia, H. (2001). Naphthalene included within all-silica zeolites: influence of the host on the naphthalene photophysics. *J. Phys. Chem. B* 105, 9973–9979.
- Márquez, F., García, H., Palomares, E., Fernández, L., and Corma, A. (2000). Spectroscopic evidence in support of the molecular orbital confinement concept: case of Anthracene Incorporated in zeolites. *J. Am. Chem. Soc.* 122, 6520–6521.
- Zicovich-Wilson, C.M., Corma, A., and Viruela, P. (1994). Electronic confinement of molecules in microscopic pores. A new concept which contributes to the explanation of the catalytic activity of zeolites. *J. Phys. Chem.* 98, 10863–10870.
- Corma, A., García, H., Sastre, G., and Viruela, P.M. (1997). Activation of molecules in confined spaces: an approach to zeolite–guest supramolecular systems. *J. Phys. Chem. B* 101, 4575–4582.
- Borgoo, A., Tozer, D.J., Geerlings, P., and De Prof, F.D. (2009). Confinement effects on excitation energies and regioselectivity as probed by the Fukui function and the molecular electrostatic potential. *Phys. Chem. Chem. Phys.* 11, 2862–2868.
- Borgoo, A., Tozer, D.J., Geerlings, P., and De Prof, F.D. (2008). Influence of confinement on atomic and molecular reactivity indicators in DFT. *Phys. Chem. Chem. Phys.* 10, 1406–1410.
- Weisz, P.B. (1980). Molecular shape selective catalysis. *Pure Appl. Chem.* 52, 2091–2103.
- Yashima, T., Yamazaki, K., Ahmad, H., Katsuta, M., and Hara, N. (1970). Alkylation on synthetic zeolites. *J. Catal.* 17, 151–156.
- Kaeding, W.W., Chu, C., Young, L.B., Weinstein, B., and Butter, S.A. (1981). Selective alkylation of toluene with methanol to produce para-xylene. *J. Catal.* 67, 159–174.
- Chirico, R.D., and Steele, W.V. (1997). Thermodynamic equilibria in xylene isomerization. 5. Xylene isomerization equilibria from thermodynamic studies and reconciliation of calculated and experimental product distributions †. *J. Chem. Eng. Data* 42, 784–790.
- Wang, H., Klein, M.G., Zou, H., Lane, W., Snell, G., Levin, I., Li, K., and Sang, B.C. (2015). Crystal structure of human stearyl-coenzyme A desaturase in complex with substrate. *Nat. Struct. Mol. Biol.* 22, 581–585.

15. Tocher, D.R., Leaver, M.J., and Hodgson, P.A. (1998). Recent advances in the biochemistry and molecular biology of fatty acyl desaturases. *Prog. Lipid Res.* 37, 73–117.
16. Paton, C.M., and Ntambi, J.M. (2009). Biochemical and physiological function of stearoyl-CoA desaturase. *Am. J. Physiol. Endocrinol. Metab.* 297, E28–E37.
17. Nagai, J., and Bloch, K. (1965). Synthesis of oleic acid by *Euglena gracilis*. *J. Biol. Chem.* 240, 3702–3703.
18. Wendt, K.U., Lenhart, A., and Schulz, G.E. (1999). The structure of the membrane protein squalene-hopene cyclase at 2.0 Å resolution. *J. Mol. Biol.* 286, 175–187.
19. Landis, P.S., and Venuto, P.B. (1966). Organic reactions catalyzed by crystalline aluminosilicates IV. Beckmann rearrangement of ketoximes to amides. *J. Catal.* 6, 245–252.
20. Venuto, P.B., and Landis, P.S. (1966). Organic reactions catalyzed by crystalline aluminosilicates III. Condensation reactions of carbonyl compounds. *J. Catal.* 6, 237–244.
21. Venuto, P., Hamilton, L., Landis, P., and Wise, J. (1966). Organic reactions catalyzed by crystalline aluminosilicates I. Alkylation reactions. *J. Catal.* 5, 81–98.
22. Nagarajan, V., Mohanty, A.K., and Misra, M. (2016). Perspective on polylactic acid (PLA) based sustainable materials for durable applications: focus on toughness and heat resistance. *ACS Sustain. Chem. Eng.* 4, 2899–2916.
23. Dusselier, M., Van Wouwe, P.V., Dewaele, A., Jacobs, P.A., and Sels, B.F. (2015). Shape-selective zeolite catalysis for bioplastics production. *Science* 349, 78–80.
24. Corma, A., Nemeth, L.T., Renz, M., and Valencia, S. (2001). Sn-zeolite beta as a heterogeneous chemoselective catalyst for Baeyer–Villiger oxidations. *Nature* 412, 423–425.
25. Farrusseng, D., Aguado, S., and Pinel, C. (2009). Metal-organic frameworks: opportunities for catalysis. *Angew. Chem. Int. Ed.* 48, 7502–7513.
26. Rogge, S.M.J., Bavykina, A., Hajek, J., Garcia, H., Olivos-Suarez, A.I., Sepúlveda-Escribano, A., Vimont, A., Clet, G., Bazin, P., Kapteijn, F., et al. (2017). Metal-organic and covalent organic frameworks as single-site catalysts. *Chem. Soc. Rev.* 46, 3134–3184.
27. Ma, L., Abney, C., and Lin, W. (2009). Enantioselective catalysis with homochiral metal-organic frameworks. *Chem. Soc. Rev.* 38, 1248–1256.
28. Heitbaum, M., Glorius, F., and Escher, I. (2006). Asymmetric heterogeneous catalysis. *Angew. Chem. Int. Ed.* 45, 4732–4762.
29. Metrano, A.J., and Miller, S.J. (2019). Peptide-Based Catalysts Reach the Outer Sphere through Remote Desymmetrization and Atroposelectivity. *Acc. Chem. Res.* 52, 199–215.
30. Breslow, R., and Campbell, P. (1969). Selective aromatic substitution within a cyclodextrin mixed complex. *J. Am. Chem. Soc.* 91, 3085.
31. Breslow, R., and Overman, L.E. (1970). An “artificial enzyme” combining a metal catalytic group and a hydrophobic binding cavity. *J. Am. Chem. Soc.* 92, 1075–1077.
32. Breslow, R. (1995). Biomimetic chemistry and artificial enzymes: catalysis by design. *Acc. Chem. Res.* 28, 146–153.
33. Breslow, R., and Dong, S.D. (1998). Biomimetic reactions catalyzed by cyclodextrins and their derivatives. *Chem. Rev.* 98, 1997–2012.
34. Mouarrawis, V., Plessius, R., van der Lugt, J.I., and Reek, J.N.H. (2018). Confinement effects in catalysis using well-defined materials and cages. *Front. Chem.* 6, 623.
35. Grommet, A.B., Feller, M., and Klajn, R. (2020). Chemical reactivity under nanoconfinement. *Nat. Nanotechnol.* 15, 256–271.
36. Caulder, D.L., Powers, R.E., Parac, T.N., and Raymond, K.N. (1998). The self-assembly of a predesigned tetrahedral M4L6 supramolecular cluster. *Angew. Chem. Int. Ed.* 37, 1840–1843.
37. Pluth, M.D., Bergman, R.G., and Raymond, K.N. (2007). Acid catalysis in basic solution: a supramolecular host promotes orthoformate hydrolysis. *Science* 316, 85–88.
38. Dong, V.M., Fiedler, D., Carl, B., Bergman, R.G., and Raymond, K.N. (2006). Molecular recognition and stabilization of iminium ions in water. *J. Am. Chem. Soc.* 128, 14464–14465.
39. Hastings, C.J., Pluth, M.D., Bergman, R.G., and Raymond, K.N. (2010). Enzymelike catalysis of the Nazarov cyclization by supramolecular encapsulation. *J. Am. Chem. Soc.* 132, 6938–6940.
40. Hastings, C.J., Backlund, M.P., Bergman, R.G., and Raymond, K.N. (2011). Enzyme-like control of carbocation deprotonation regioselectivity in supramolecular catalysis of the Nazarov cyclization. *Angew. Chem. Int. Ed.* 50, 10570–10573.
41. Hart-Cooper, W.M., Clary, K.N., Toste, F.D., Bergman, R.G., and Raymond, K.N. (2012). Selective monoterpene-like cyclization reactions achieved by water exclusion from reactive intermediates in a supramolecular catalyst. *J. Am. Chem. Soc.* 134, 17873–17876.
42. Takezawa, H., Kanda, T., Nanjo, H., and Fujita, M. (2019). Site-selective functionalization of linear diterpenoids through U-shaped folding in a confined artificial cavity. *J. Am. Chem. Soc.* 141, 5112–5115.
43. Zhang, Q., and Tiefenbacher, K. (2015). Terpene cyclization catalysed inside a self-assembled cavity. *Nat. Chem.* 7, 197–202.
44. Zhang, Q., Rinkel, J., Goldfuss, B., Dickschat, J.S., and Tiefenbacher, K. (2018). Sesquiterpene cyclisations catalysed inside the resorcinarene capsule and application in the short synthesis of isolongifolene and isolongifolenone. *Nat. Catal.* 1, 609–615.
45. Zhang, Q., and Tiefenbacher, K. (2019). Sesquiterpene cyclizations inside the hexameric resorcinarene capsule: total synthesis of  $\delta$ -selinene and mechanistic studies. *Angew. Chem. Int. Ed.* 58, 12688–12695.
46. Syntirivanis, L.D., Némethová, I., Schmid, D., Levi, S., Prescimone, A., Bissegger, F., Major, D.T., and Tiefenbacher, K. (2020). Four-step access to the sesquiterpene natural product presilphiperfolan-1 $\beta$ -ol and unnatural derivatives via supramolecular catalysis. *J. Am. Chem. Soc.* 142, 5894–5900.
47. Fiedler, D., Bergman, R.G., and Raymond, K.N. (2004). Supramolecular catalysis of a unimolecular transformation: aza-cope rearrangement within a self-assembled host. *Angew. Chem. Int. Ed.* 43, 6748–6751.
48. MacGillivray, L.R., and Atwood, J.L. (1997). A chiral spherical molecular assembly held together by 60 hydrogen bonds. *Nature* 389, 469–472.
49. Lesburg, C.A., Zhai, G., Cane, D.E., and Christianson, D.W. (1997). Crystal structure of pentalenene synthase: mechanistic insights on terpenoid cyclization reactions in biology. *Science* 277, 1820–1824.
50. Starks, C.M., Back, K., Chappell, J., and Noel, J.P. (1997). Structural basis for cyclic terpene biosynthesis by tobacco 5-epi-aristolochene synthase. *Science* 277, 1815–1820.
51. Christianson, D.W. (2017). Structural and chemical biology of terpenoid cyclases. *Chem. Rev.* 117, 11570–11648.
52. Christianson, D.W. (2006). Structural biology and chemistry of the terpenoid cyclases. *Chem. Rev.* 106, 3412–3442.
53. Zhang, Q., and Tiefenbacher, K. (2013). Hexameric resorcinarene capsule is a Brønsted acid: investigation and application to synthesis and catalysis. *J. Am. Chem. Soc.* 135, 16213–16219.
54. Hatano, M., Mizuno, T., Izumiseki, A., Usami, R., Asai, T., Akakura, M., and Ishihara, K. (2011). Enantioselective Diels–Alder reactions with anomalous endo/exo selectivities using conformationally flexible chiral supramolecular catalysts. *Angew. Chem. Int. Ed.* 50, 12189–12192.
55. Hatano, M., and Ishihara, K. (2012). Conformationally flexible chiral supramolecular catalysts for enantioselective Diels–Alder reactions with anomalous endo/exo selectivities. *Chem. Commun. (Camb.)* 48, 4273–4283.
56. Hatano, M., Sakamoto, T., Mizuno, T., Goto, Y., and Ishihara, K. (2018). Chiral supramolecular U-shaped catalysts induce the multiselective Diels–Alder reaction of propargyl aldehyde. *J. Am. Chem. Soc.* 140, 16253–16263.
57. For example, Lin and coworkers showed in 2013 that the incorporation of chiral phosphoric acids in a MOF is accompanied with a reversal of the enantioselectivity in a Brønsted acid-catalyzed Friedel–Crafts reaction of indole with N-sulfonyl aldimines. The authors suggest that the confinement of the surrounding second coordination sphere created by the MOF is responsible for the observed switch in the preferred enantiomer. Zheng, M., Liu, Y., Wang, C., Liu, S., and Lin, W. (2012). Cavity-induced enantioselectivity reversal in a chiral metal-organic framework Brønsted acid catalyst. *Chem. Sci.* 3, 2623–2627.
58. Maruoka, K., Itoh, T., Sakurai, M., Nonoshita, K., and Yamamoto, H. (1988). Amphiphilic reactions by means of exceptionally bulky organoaluminum reagents. Rational approach

- for obtaining unusual equatorial, anti-Cram, and 1,4 selectivity in carbonyl alkylation. *J. Am. Chem. Soc.* **110**, 3588–3597.
59. Maruoka, K., Itoh, T., and Yamamoto, H. (1985). Methylaluminum bis(2,6-di-tert-butyl-4-alkylphenoxide). A new reagent for obtaining unusual equatorial and anti-Cram selectivity in carbonyl alkylation. *J. Am. Chem. Soc.* **107**, 4573–4576.
60. Maruoka, K., Imoto, H., and Yamamoto, H. (1994). Exo-selective Diels-Alder reaction based on a molecular recognition approach. *J. Am. Chem. Soc.* **116**, 12115–12116.
61. Maruoka, K., Saito, S., and Yamamoto, H. (1992). Discrimination of two different ester carbonyls with methylaluminum bis(2,6-di-tert-butyl-4-methylphenoxide). Application to the regiocontrolled and stereocontrolled Diels-Alder reaction of unsymmetrical fumarates. *J. Am. Chem. Soc.* **114**, 1089–1090.
62. Maruoka, K., Imoto, H., Saito, S., and Yamamoto, H. (1994). Virtually complete blocking of  $\alpha,\beta$ -unsaturated aldehyde carbonyls by complexation with aluminum tris(2,6-diphenylphenoxide). *J. Am. Chem. Soc.* **116**, 4131–4132.
63. Kutateladze, D.A., Strassfeld, D.A., and Jacobsen, E.N. (2020). Enantioselective tail-to-head cyclizations catalyzed by dual-hydrogen-bond donors. *J. Am. Chem. Soc.* **142**, 6951–6956.
64. Seayad, J., Seayad, A.M., and List, B. (2006). Catalytic asymmetric Pictet–Spengler reaction. *J. Am. Chem. Soc.* **128**, 1086–1087.
65. Gatzmeier, T., van Gemmeren, M., Xie, Y., Höfler, D., Leutzsch, M., and List, B. (2016). Asymmetric Lewis acid organocatalysis of the Diels–Alder reaction by a silylated C–H acid. *Science* **351**, 949–952.
66. Hentges, S.G., and Sharpless, K.B. (1980). Asymmetric induction in the reaction of osmium tetroxide with olefins. *J. Am. Chem. Soc.* **102**, 4263–4265.
67. Sharpless, K.B., Amberg, W., Bennani, Y.L., Crispino, G.A., Hartung, J., Jeong, K.S., Kwong, H.L., Morikawa, K., and Wang, Z.M. (1992). The osmium-catalyzed asymmetric dihydroxylation: a new ligand class and a process improvement. *J. Org. Chem.* **57**, 2768–2771.
68. Amberg, W., Bennani, Y.L., Chadha, R.K., Crispino, G.A., Davis, W.D., Hartung, J., Jeong, K.S., Ogino, Y., Shibata, T., and Sharpless, K.B. (1993). Syntheses and crystal structures of the cinchona alkaloid derivatives used as ligands in the osmium-catalyzed asymmetric dihydroxylation of olefins. *J. Org. Chem.* **58**, 844–849.
69. Corey, E.J., Noe, M.C., and Guzman-Perez, A. (1995). Catalytic enantioselective synthesis of (14R)-14-hydroxy-4,14-retro-retinol from retinyl acetate. *Tetrahedron Lett.* **36**, 4171–4174.
70. Corey, E.J., Noe, M.C., and Sarshar, S. (1994). X-ray crystallographic studies provide additional evidence that an enzyme-like binding pocket is crucial to the enantioselective dihydroxylation of olefins by OsO<sub>4</sub>–bis-cinchona alkaloid complexes. *Tetrahedron Lett.* **35**, 2861–2864.
71. Corey, E.J., and Noe, M.C. (1996). Kinetic investigations provide additional evidence that an enzyme-like binding pocket is crucial for high enantioselectivity in the bis-cinchona alkaloid catalyzed asymmetric dihydroxylation of olefins. *J. Am. Chem. Soc.* **118**, 319–329.
72. Kolb, H.C., Andersson, P.G., and Sharpless, K.B. (1994). Toward an understanding of the high enantioselectivity in the osmium-catalyzed asymmetric dihydroxylation (AD). 1. Kinetics. *J. Am. Chem. Soc.* **116**, 1278–1291.
73. Ćorić, I., and List, B. (2012). Asymmetric spiroacetalization catalysed by confined Brønsted acids. *Nature* **483**, 315–319.
74. Klussmann, M., Ratjen, L., Hoffmann, S., Wakchaure, V., Goddard, R., and List, B. (2010). Synthesis of TRIP and analysis of phosphate salt impurities. *Synlett* **2010**, 2189–2192.
75. Kaib, P.S.J., Schreyer, L., Lee, S., Properzi, R., and List, B. (2016). Extremely active organocatalysts enable a highly enantioselective addition of allyltrimethylsilane to aldehydes. *Angew. Chem. Int. Ed.* **55**, 13200–13203.
76. Yagupolskii, L.M., Petrik, V.N., Kondratenko, N.V., Sooväli, L., Kaljurand, I., Leito, I., and Koppel, I.A. (2002). The immense acidifying effect of the supersubstituent = NSO<sub>2</sub>CF<sub>3</sub> on the acidity of amides and amidines of benzoic acids in acetonitrile. *J. Chem. Soc. Perkin Trans. 2* **2002**, 1950–1955.
77. Yepes, D., Neese, F., List, B., and Bistoni, G. (2020). Unveiling the delicate balance of steric and dispersion interactions in organocatalysis using high-level computational methods. *J. Am. Chem. Soc.* **142**, 3613–3625.
78. Gatzmeier, T., Turberg, M., Yepes, D., Xie, Y., Neese, F., Bistoni, G., and List, B. (2018). Scalable and highly diastereo- and enantioselective catalytic Diels–Alder reaction of  $\alpha,\beta$ -unsaturated methyl esters. *J. Am. Chem. Soc.* **140**, 12671–12676.
79. Schreyer, L., Kaib, P.S.J., Wakchaure, V.N., Obradors, C., Properzi, R., Lee, S., and List, B. (2018). Confined acids catalyze asymmetric single aldolizations of acetaldehyde enolates. *Science* **362**, 216–219.
80. Ouyang, J., Kennemur, J.L., De, C.K., Farès, C., and List, B. (2019). Strong and confined acids enable a catalytic asymmetric Nazarov cyclization of simple divinyl ketones. *J. Am. Chem. Soc.* **141**, 3414–3418.
81. Tsuji, N., Kennemur, J.L., Buyck, T., Lee, S., Prévost, S., Kaib, P.S.J., Bykov, D., Farès, C., and List, B. (2018). Activation of olefins via asymmetric Brønsted acid catalysis. *Science* **359**, 1501–1505.
82. Boxer, M.B., and Yamamoto, H. (2006). Tris(trimethylsilyl)silyl-governed aldehyde cross-aldol cascade reaction. *J. Am. Chem. Soc.* **128**, 48–49.
83. Boxer, M.B., and Yamamoto, H. (2007). “Super silyl” group for diastereoselective sequential reactions: access to complex chiral architecture in one pot. *J. Am. Chem. Soc.* **129**, 2762–2763.
84. Gatzmeier, T., Kaib, P.S.J., Lingnau, J.B., Goddard, R., and List, B. (2018). The catalytic Asymmetric Mukaiyama–Michael reaction of silyl ketene acetals with  $\alpha,\beta$ -unsaturated methyl esters. *Angew. Chem. Int. Ed.* **57**, 2464–2468.